

The charge transport mechanism and electron trap nature in thermal oxide on silicon

Damir R. Islamov,^{1,2, a)} Vladimir A. Gritsenko,^{1,2} Timofey V. Perevalov,^{1,2} Oleg M. Orlov,^{3, b)} and Gennady Ya. Krasnikov³

¹⁾*Rzhanov Institute of Semiconductor Physics, Siberian Branch of the Russian Academy of Sciences, Novosibirsk 630090, Russian Federation*

²⁾*Novosibirsk State University, Novosibirsk 630090, Russian Federation*

³⁾*JSC Molecular Electronics Research Institute, Zelenograd, Moscow 124460, Russian Federation*

(Dated: 27 March 2018)

The charge transport mechanism of electron via traps in amorphous SiO₂ has been studied. Electron transport is limited by phonon-assisted tunneling between traps. Thermal and optical trap energies $W_t = 1.6$ eV, $W_{opt} = 3.2$ eV, respectively, were determined. Charge flowing leads to oxygen vacancies generation, and the leakage current increases due to the increase of charge trap density. Long-time annealing at high temperatures decreased the leakage current to initial values due to oxygen vacancies recombination with interstitial oxygen. It is found that the oxygen vacancies act as electron traps in SiO₂.

PACS numbers: 72.20.Jv, 77.55.df, 73.50.-h, 72.10.Di

Keywords: silica, oxygen vacancy, traps, charge transport, leakage current.

Silica SiO₂ is the key material in electronic and optical devices, fibers. Intrinsic defects in SiO₂ act as localization centers for electrons and holes (traps). The presence of such defects in particular layers of a device results in the whole device degradation. The main intrinsic defects in SiO₂ are threefold coordinated silicon atom with an unpaired electron (Si.)¹⁻³, the oxygen vacancy (Si-Si bond)⁴⁻⁹, non-bridging oxygen (Si-O.)^{4,10}, peroxide radical (Si-O-O.)^{4,6} and a peroxide bridge (Si-O-O-Si)⁴. Here the sign (-) shows a chemical bond formed by two electrons, the sign (.) denotes an unpaired electron. On the base of numerous experiments it was found that oxygen vacancies in SiO₂ act as traps for holes^{6,9,11}. According to the results of quantum-chemical simulations, it was predicted that the oxygen vacancy can act as traps for electrons^{10,12}. However, the electron trapping energy and the trap ionization mechanism in strong electric field are unknown.

Long-time charge flowing through SiO₂ in a strong electric field ($F \approx 10^7$ V/cm) leads to the oxide conductivity increase at lower electric field values ($\approx 2 \times 10^6$ V/cm). Thus, an extra current through the dielectric is added to the Fowler-Nordheim tunneling current^{13,14}, and addition values are comparable to the tunneling ones. This phenomenon is called Stress Induced Leakage Current (SILC)⁴⁻⁷. Despite the fact that SILC is studied widely, both experimentally and theoretically¹⁵⁻¹⁸, the nature of the defects responsible for SILC and charge transport mechanism are still debatable questions. The purposes of the present study are identification of the ionization mechanism of electron traps in SiO₂ in external electric field and determination of the trap parameters

(ionization energy, concentration). The phenomenon of SILC was used to generate the traps in SiO₂ followed by a charge transport study.

SILC and transport measurements were performed on FET transistors with the floating gate, manufactured using the 180 nm design rule technology. The *p*-Si substrate was used as the bottom contact, the *n*⁺-type *poly*-Si floating gate was used as the top contact. The tunnel SiO₂ layer thickness was 7.5 nm. Test samples were formed of 16 parallel-connected *n*-Si/SiO₂/*poly*-Si capacitors with the total area of the *poly*-silicon electrodes of $8 \times 10^4 \mu\text{m}^2$. SILC was generated by the current of 1 mA/cm². The total value of the flown charge via tunnel SiO₂ was 0.01–10 C/cm². Transport measurements have been performed at temperatures of 25–70 °C.

Simulation was conducted for a 72-atom α -SiO₂ supercell with the Quantum-ESPRESSO software within the scope of the density functional theory with B3LYP hybrid functional¹⁹. This method yields the α -SiO₂ band gap of 8.0 eV, in excellent agreement with the experimental value²⁰ and with the theoretical value of 8.1 eV obtained for amorphous SiO₂ within framework of similar approach³. See supplemental material at²¹ for detailed description of the numeric simulation procedure. [give brief description of material]. Electron and hole trap energies W_t^e and W_t^h at the Si-Si bond are evaluated as difference between perfect and defect supercell electron affinities and ionization energies as follows:

$$W_t^{e/h} = E_p^{+1/-1} - E_d^{+1/-1} - E_p^0 + E_d^0. \quad (1)$$

Here $E_p^{0/+1/-1}$ and $E_d^{0/+1/-1}$ represent the values for the total energy of an ideal and defect supercell with a different amount of the total charge. This approach was proposed for SiO₂ to obtain the defect level positions between different charge states²², and used for charge localization energy calculation in Si₃N₄²³ and HfO₂²⁴.

^{a)}Electronic mail: damir@isp.nsc.ru

^{b)}Electronic mail: oorlov@mikron.ru

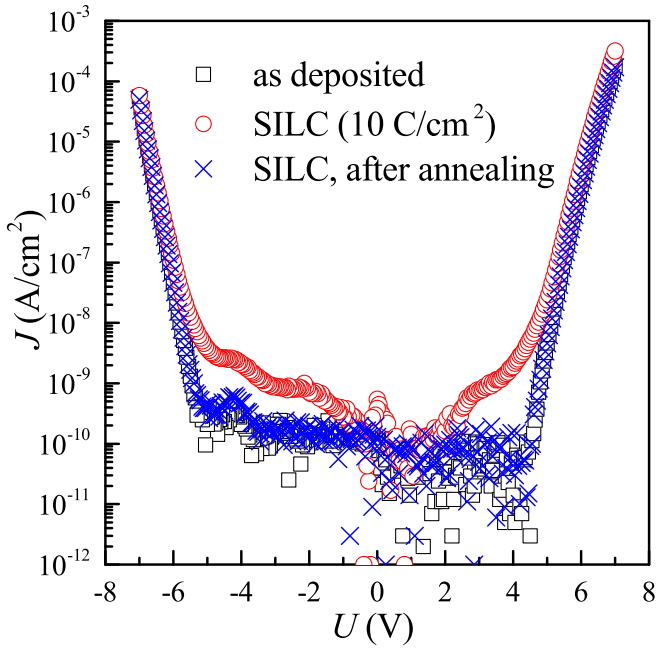


FIG. 1: (Color online) Experimental current-voltage characteristics of n -Si/SiO₂/ $poly$ -Si structures at room temperature (25 °C) before SILC (\square), after SILC (\circ), and after SILC followed by long-time annealing (\times).

Experimental current-voltage characteristics (J - V) of the as deposited oxide are shown in Fig. 1 by box symbols. At high voltages $|U| > 5$ V ($F > 6$ MV/cm) the current depends on the voltage exponentially and is limited by the tunnelling emission that proceeds by the Fowler-Nordheim mechanism¹³:

$$J_{\text{FN}} = AF^2 \exp\left(-\frac{B\sqrt{m^*}\Phi_0^{3/2}}{F}\right), \quad (2)$$

$$A = \frac{e^3}{8\pi h\Phi_0}, B = \frac{8\pi\sqrt{2}}{3he},$$

where J_{FN} is the tunneling current density, m^* is the electron effective tunneling mass, Φ_0 is the height of the triangular potential barrier for electrons at the Si/SiO₂ interface, e is the elementary (electron) charge, h is the Planck constant. When $|U| < 5$ V, the measured current values will be determined by the sensitivity of the measuring devices and bulk properties of the substrate. According to photo emission measurements, the height of the triangular potential barrier for electrons at the Si/SiO₂ interface is $\Phi = 3.14$ eV²⁵. The electron energy spectrum quantization in high fields at the Si/SiO₂ interface leads to a decrease of the effective barrier height to $\Phi_0 = 2.9$ eV²⁶. Taking $\Phi_0 = 2.9$ eV for simulations of experimental data with Eq. (2), we get the electron effective mass in SiO₂ $m^*/m_e = 0.5 \pm 0.02$ at both positive and negative biases on the $poly$ -Si electrode. These results are in consistent with the literature^{26,27}

The experimental J - V characteristics after SILC (10 C/cm²) are shown in Fig. 1 by round symbols. At high bias $|U| > 5$ V on the $poly$ -Si contact, the cur-

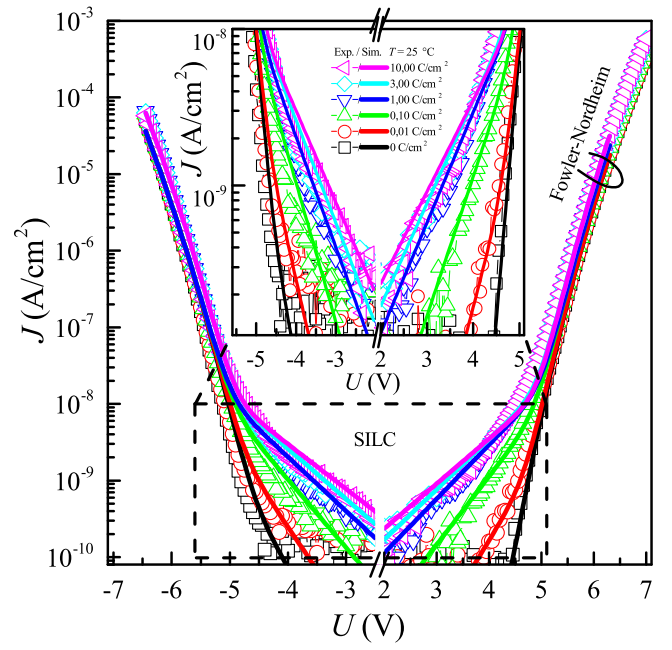


FIG. 2: (Color online) Experimental (characters) and calculated (lines) current-voltage characteristics of n -Si/SiO₂/ $poly$ -Si structures at room temperature (25 °C) after different SILC stress. Calculations were done using Eq. (6). The inset: SILC mode.

rent through SiO₂ films is limited by Fowler-Nordheim tunneling. The current at lower voltages $|U| < 5$ V is controlled by SILC. The characters in Fig. 2 represent the experimental J - V characteristics of n -Si/SiO₂/ $poly$ -Si structures at room temperature after different SILC stresses. The SILC currents ($2.5 \text{ V} < |U| < 5 \text{ V}$) grow with the increasing SILC stress. The slope of J - V curves at low voltages decreases if the SILC is increased. The temperature increase leads to growing SILC currents on 30–50%, but Fowler-Nordheim tunneling.

When the trap density is high and the distance between them is short enough, trapped electrons can tunnel between the neighboring traps without ionization to the conduction band²⁸.

A diagram of the electron tunneling from a phonon-bound trap to the other one at a distance of a in the presence of an external electric field is shown in Fig. 3. The energy dependencies from generalized coordinate Q of a system trapped-electron-bound-with-phonon are shown by $U_b(Q)$ terms. The $U_f(Q)$ terms correspond to “free” electrons in the conduction band. Solid lines represent the initial, before the tunneling state, dashed lines represent the final state after tunneling. Due to the external electric field electrons on the neighboring traps have different energy levels (slanted lines $\varepsilon(Q)$), and the tunnel transition must be accompanied by inelastic processes, like phonon emission and phonon absorption, in order to compensate the energy difference. The phonon-assisted tunneling model²⁸ takes into account this circumstance.

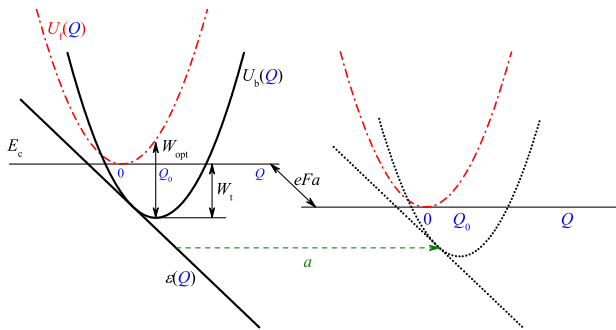


FIG. 3: (Color online) Configuration diagram for two phonon-coupled traps. $U_f(Q)$ is the potential energy of an empty oscillator (without trapped electron); $U_b(Q)$ is the potential energy of an occupied oscillator (with trapped electron); $\epsilon(Q)$ is the position of the energy level of the trapped electron dependent on coordinate Q ; and E_c is the conduction-band edge. The solid and dotted lines refer to the initially occupied and empty state, respectively. The most probable tunneling transition for the electron when both oscillators take position $Q_0/2$ is shown by the horizontal dashed arrow.

According to this model, the rate of such transitions is given by

$$P_{\text{tun}} = \frac{2\sqrt{\pi}\hbar W_t}{m^*a^2Q_0\sqrt{kT}} \exp\left(-\frac{2a\sqrt{2m^*W_t}}{\hbar}\right) \times \exp\left(-\frac{W_{\text{opt}} - W_t}{2kT}\right) \sinh\left(\frac{eFa}{2kT}\right). \quad (3)$$

Here $\hbar = h/2\pi$, $Q_0 = \sqrt{2(W_{\text{opt}} - W_t)}$, W_t and W_{opt} are thermal and optical trap energies, k in the Boltzmann constant, T is the temperature. At high temperatures, the charge transport through the dielectrics is described within monopolar model involving Shockley-Read-Hall equations and the Poisson equation:

$$\frac{\partial n_t}{\partial t} = \frac{1}{e} \nabla \cdot \mathbf{J} - a \nabla \cdot \left(n_t \left(1 - \frac{n_t}{N} \right) P_{\text{tun}} \frac{\mathbf{F}}{|\mathbf{F}|} \right), \quad (4)$$

$$\nabla \cdot \mathbf{F} = -\frac{en_t}{\epsilon\epsilon_0},$$

where n_t is the filled trap density, t is time, $N = a^{-3}$ is the trap density, \mathbf{J} is the current density, ϵ is the static SiO_2 permittivity ($\epsilon = 3.9$), ϵ_0 is the electric constant. In the static one-dimensional case, Eq. (4) gives the current-voltage characteristics

$$J_{\text{tun}} = \frac{e}{a^2} \frac{n_t}{N} \left(1 - \frac{n_t}{N} \right) P_{\text{tun}}. \quad (5)$$

Note, the tunneling current takes a maximum value at $n_t/N = 1/2$. Taking into account Fowler-Nordheim tunneling (2), one can get the total current-voltage characteristics

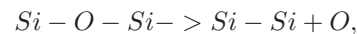
$$J = \frac{s}{S} J_{\text{tun}} + J_{\text{FN}}, \quad (6)$$

where J is the total current density, S is the total sample square ($8 \times 10^4 \mu\text{m}^2$), s is the square of SILC area. We assume that charge stress induces extra traps on a part of the SiO_2 layer. This stressed part, having effective square of s , shunts the whole sample, and gives additive to the current.

The comparison of experimental data (characters) with the theory (6) (lines) is presented in Fig. 2. As a result, we obtained thermal and optical trap energies in SiO_2 $W_t = 1.6 \text{ eV}$ and $W_{\text{opt}} = 3.2 \text{ eV}$, respectively. Simulations of experimental current-voltage characteristics measures at 70°C gives the same trap energy values. Simulations within well-known Frenkel model of isolated Coulomb center ionization^{29,30} predict that dynamic permittivity increases with the charge stress up to $\epsilon_\infty = 30$, that is physically incorrect results. All above confirm that using the model of the phonon-assisted tunneling between traps is correct. The obtained model parameter values including trap densities N and the squares of SILC area s depending on the total SILC charge Σ are given in Table I.

We should note that the multi-phonon charge transport model in the SILC mode was introduced earlier^{16,17}. This model is not analytical, and it requires complex numerical calculations to describe the SILC transport.

We assume that oxygen vacancies (Si-Si bonds) act as traps responsible for SILC in SiO_2 , which are generated as



where O is the interstitial oxygen atom. The electronic structure of Si-Si bonds in SiO_2 has been studied intensively^{4,8,9,11}. The trap energies for electrons and holes, calculated from the first principles (1), are 1.2 eV and 1.6 eV, respectively. The Si-Si bond in silicon oxide acts as an amphoteric trap capable of both electron and hole capturing. Taking into account that such calculations usually underestimate electron trap energy values, one can conclude that the *ab initio* simulation results agree to the thermal trap energy value of 1.6 eV obtained from transport simulations.

It is interesting to compare thermal trap energy $W_t = 1.6 \text{ eV}$ in SiO_2 to the Stokes shift of Si-Si defect luminescence. It is known that Si-Si bonds exhibit the ultraviolet luminescence band with the photon energy of 4.4 eV^{9,31}. The excitation maximum of this band is located at 7.6 eV^{8,9,31}. A half of the Stokes luminescence shift $(7.6 - 4.4)/2 = 1.6 \text{ eV}$ is equal to the energy of electron and hole traps in SiO_2 , which are Si-Si bonds¹¹. This value is equal to the W_t value obtained from charge transport in SiO_2 experiments in the SILC mode. Thus, one can conclude that, namely, oxygen vacancies act as the charge traps in SiO_2 after the SILC stress.

Note that the obtained optical energy value W_{opt} is twice bigger than thermal trap energy W_t . This empirical rule of the multiphonon transport mechanism is executed for other dielectrics^{27,32-35}. To confirm or refute universal nature of this correlation, it is necessary to collect

TABLE I: Obtained values of parameter (2), (3), (5), (6).

Σ (C/cm ²)	0	0.01	0.1	1	3	10
W_t (eV)				1.6		
W_{opt} (eV)				3.2		
m^*/m_e				0.5 ± 0.02		
N (cm ⁻³)	$\ll 10^{20}$	1×10^{21}	2×10^{21}	4×10^{21}	5×10^{21}	7×10^{21}
s (nm ²)	0	25×10^2	1×10^4	1.5×10^4	2×10^4	3×10^4

statistics for a large number of dielectrics. The optical trap energy $W_{opt} = 3.2$ eV evaluated from the transport measurement is very close to the electron trap energy of 3.1 eV defined from the tunneling discharge of trapped in SiO₂ electrons³⁶.

Taking into account arguments above, one can conclude that namely oxygen vacancies are responsible for the SILC phenomenon, but not other defects in SiO₂.

After the SILC stress some samples were treated by annealing at the temperature of 250 °C during 120 hours. A comparison of the current-voltage characteristics measures for the “as deposited”, after the SILC stress and after annealing structures are shown in Fig. 1. One can see that J - V curves, after annealing, are almost identical to the “as deposited” control ones. This phenomenon demonstrates that long-time annealing leads to the electronic structure of the tunnel SiO₂, which is identical to one of the “as deposited” films. This means that the trap density decreases with annealing down to initial values. This phenomenon makes it possible to controllably suppress the leakage currents caused by the tunnel SiO₂ degradation due to the SILC stress.

In conclusion, the electron transport due to the traps in SiO₂ was studied experimentally. It was demonstrated that the transport is limited by phonon-assisted tunneling between traps. Comparison trap energy values obtained from different experiments on charge transport in SiO₂, luminescence of oxygen vacancy (Si–Si bond) in SiO₂, and *ab initio* simulations of Si–Si bond electronic structure, it was found that the oxygen vacancies (Si–Si bonds) act as the charge localization centers (traps) in SiO₂. The SILC stress leads to oxygen vacancies generation. The thermal and optical trap energies were evaluated. Long-time annealing at 250 °C results in the recombination of oxygen vacancies and interstitial oxygen, and reduces the leakage current to the initial level.

This work was supported by the Russian Science Foundation (grant #16-19-00002). The computations have been carried out at the computational cluster in the Rzhzanov Institute of Semiconductor Physics SB RAS.

¹M. Boero, A. Pasquarello, J. Sarnthein, and R. Car, *Physical Review Letters* **78**, 887 (1997).

²A.-M. El-Sayed, M. B. Watkins, T. Grasser, V. V. Afanas'ev, and A. L. Shluger, *Physical Review Letters* **114**, 115503 (2015).

³A.-M. El-Sayed, Y. Wimmer, W. Goes, T. Grasser, V. V. Afanas'ev, and A. L. Shluger, *Physical Review B* **92**, 014107 (2015).

⁴E. P. O'Reilly and J. Robertson, *Physical Review B* **27**, 3780 (1983).

⁵C.-L. Kuo and G. S. Hwang, *Physical Review Letters* **97**, 066101 (2006).

⁶L. Giordano, P. V. Sushko, G. Pacchioni, and A. L. Shluger, *Physical Review B* **75**, 024109 (2007).

⁷S. Agnello, R. Boscaino, M. Cannas, F. M. Gelardi, M. Leone, and B. Boizot, *Physical Review B* **67**, 033202 (2003).

⁸R. Tohmon, Y. Shimogaichi, H. Mizuno, Y. Ohki, K. Nagasawa, and Y. Hama, *Physical Review Letters* **62**, 1388 (1989).

⁹G. Pacchioni and G. Ierañ, *Physical Review Letters* **79**, 753 (1997).

¹⁰L. Giordano, P. V. Sushko, G. Pacchioni, and A. L. Shluger, *Physical Review Letters* **99**, 136801 (2007).

¹¹V. Gritsenko and H. Wong, *Critical Reviews in Solid State and Materials Sciences* **36**, 129 (2011).

¹²P. V. Sushko, S. Mukhopadhyay, A. M. Stoneham, and A. L. Shluger, *Microelectronic Engineering* **80**, 292 (2005).

¹³R. H. Fowler and L. Nordheim, *Proceedings of the Royal Society of London A: Mathematical, Physical and Engineering Sciences* **119**, 173 (1928).

¹⁴S. M. Sze and K. K. Ng, *Physics of Semiconductor Devices*, 3rd ed. (Wiley, New York, 2006) p. 832.

¹⁵P. E. Blöchl and J. H. Stathis, *Physical Review Letters* **83**, 372 (1999).

¹⁶T. Endoh, T. Chiba, H. Sakuraba, M. Lenski, and F. Masuoka, *Journal of Applied Physics* **86**, 2095 (1999).

¹⁷F. Jiménez-Molinos, A. Palma, F. Gámiz, J. Banqueri, and J. A. López-Villanueva, *Journal of Applied Physics* **90**, 3396 (2001).

¹⁸K. Komiya and Y. Omura, *Journal of Applied Physics* **92**, 2593 (2002).

¹⁹P. Giannozzi, S. Baroni, N. Bonini, M. Calandra, R. Car, C. Cavazzoni, D. Ceresoli, G. L. Chiarotti, M. Cococcioni, I. Dabo, A. Dal Corso, S. de Gironcoli, S. Fabris, G. Fratesi, R. Gebauer, U. Gerstmann, C. Gougoussis, A. Kokalj, M. Lazzeri, L. Martin-Samos, N. Marzari, F. Mauri, R. Mazzarello, S. Paolini, A. Pasquarello, L. Paulatto, C. Sbraccia, S. Scandolo, G. Sclauzero, A. P. Seitsonen, A. Smogunov, P. Umari, and R. M. Wentzcovitch, *Journal of Physics: Condensed Matter* **21**, 395502 (2009).

²⁰R. Williams, *Physical Review* **140**, A569 (1965).

²¹See supplementary material <http://dx.doi.org/10.1063/1.4960156> for the detailed description of the numeric simulation procedure.

²²A. X. Chu and W. B. Fowler, *Physical Review B* **41**, 5061 (1990).

²³M. Petersen and Y. Roizin, *Applied Physics Letters* **89**, 053511 (2006).

²⁴A. S. Foster, F. Lopez Gejo, A. L. Shluger, and R. M. Nieminen, *Physical Review B* **65**, 174117 (2002).

²⁵V. A. Gritsenko, K. P. Mogil'nikov, and A. V. Rzhzanov, *JETP Letters* **27**, 375 (1978).

²⁶Z. A. Weinberg, *Journal of Applied Physics* **53**, 5052 (1982).

²⁷K. A. Nasyrov, S. S. Shaimeev, V. A. Gritsenko, and J. H. Han, *Journal of Applied Physics* **105**, 123709 (2009).

²⁸K. A. Nasyrov and V. A. Gritsenko, *Journal of Applied Physics* **109**, 093705 (2011).

²⁹J. Frenkel, *Technical Physics of the USSR* **5**, 685 (1938).

³⁰J. Frenkel, *Physical Review* **54**, 647 (1938).

³¹C. M. Gee and M. Kastner, *Physical Review Letters* **42**, 1765 (1979).

³²N. Novikov, V. A. Gritsenko, and K. A. Nasyrov, *Applied*

[Physics Letters](#) **94**, 222904 (2009).

- ³³T. V. Perevalov, O. E. Tereshenko, V. A. Gritsenko, V. A. Pustovarov, A. P. Yelisseyev, C. Park, J. H. Han, and C. Lee, [Journal of Applied Physics](#) **108**, 013501 (2010).
- ³⁴T. V. Perevalov, V. S. Aliev, V. A. Gritsenko, A. A. Saraev, V. V. Kaichev, E. V. Ivanova, and M. V. Zamoryanskaya, [Applied](#)

[Physics Letters](#) **104**, 071904 (2014).

- ³⁵D. R. Islamov, V. A. Gritsenko, C. H. Cheng, and A. Chin, [Applied Physics Letters](#) **105**, 222901 (2014), [arXiv:1409.6887 \[cond-mat.mtrl-sci\]](#).
- ³⁶K. Yamabe and Y. Miura, [Journal of Applied Physics](#) **51**, 6258 (1980).